POLITECNICO DI MILANO

School of Industrial and Information Engineering
Master of Science in Telecommunications Engineering

Non-Orthogonal Multiple Access (NOMA) for 5G Networks and Its Application in Unmanned Aerial Vehicle Assisted Communication

Supervisor: Prof. Maurizio MAGARINI

Master Thesis of: Sohini CHATTOPADHYAY
Student ID: 876136

Academic Year 2018-2019

I dedicate this work to my family, friends and my guide.

Astratto

Per prima cosa esploriamo il concetto di schema NOMA (Non-Orthogonal Multiple Access) per il futuro accesso radio per 5G e poi studiamo l'applicazione del NOMA nella comunicazione UAV (Unmanned Aerial Vehicle). In primo luogo studieremo le tecniche fondamentali per entrambi i canali di downlink e di uplink e quindi discuterò l'ottimizzazione della capacità della rete in base ai vincoli di equità. Quindi discutiamo l'impatto dei ricevitori imperfetti sulle prestazioni delle reti NOMA. Inoltre discutiamo dell'efficienza spettrale (SE) delle reti e delle sue relazioni con l'efficienza energetica (EE). Dimostriamo anche che le reti con NOMA superano gli altri schemi di accesso multiplo in termini di somma di capacità, efficienza energetica ed efficienza spettrale. I confronti delle prestazioni sono forniti anche con schemi OMA e NOMA fissi per altitudine. I risultati vengono presentati per varie regioni di destinazione e ambienti di distribuzione, cioè urbano, rurale, urbano e denso. Chiaramente, lo schema proposto raggiunge una migliore somma a una quota più bassa che riduce il dispendio energetico complessivo dell'UAV.

Abstract

First we explore the concept of Non-Orthogonal Multiple Access (NOMA) scheme for the future radio access for 5G and then we study the application of NOMA in Unmanned Aerial Vehicle (UAV) communication. We first will study the fundamental techniques for both downlink and uplink channels and then discuss optimizing the network capacity under fairness constraints. Then we discuss the impacts of imperfect receivers on the performance of NOMA networks. Furthermore we discuss the spectral efficiency (SE) of the networks and its relations with energy efficiency (EE). We also demonstrate that the networks with NOMA outperform other multiple access schemes in terms of sum capacity, Energy Efficiency and Spectral Efficiency. Performance comparisons are also provided with altitude fixed OMA and NOMA schemes. Results are presented for various target regions and deployment environments i.e., rural, urban, and dense urban. Clearly, the proposed scheme achieves better sum-rate at a lower altitude which reduces the overall energy expenditure of the UAV.

Table of Contents

List of Figures

List of tables

CHAPTER 1

1. Introduction

1.1 Background

Current cellular networks implement Orthogonal Multiple Access (OMA) techniques such as Time Division Multiple Access (TDMA), Frequency Division Multiple Access (FDMA) or Code Division Multiple Access (CDMA). However, the high demands of future radio access systems can be met none of these techniques. The characteristics of the OMA schemes are as follows:

In TDMA, the information for every user is sent in non-overlapping time slots, so that TDMA-based networks require accurate timing synchronization which can be challenging, particularly in the uplink. In FDMA such as Orthogonal Frequency Division Multiple Access (OFDMA), information for each user is assigned to a subset of subcarriers. CDMA utilizes codes in order to separate the users over the same channel. Non Orthogonal Multiple Access is fundamentally different from these multiple access schemes which provide orthogonal access to the users either in time, frequency, code or space.

1.2 Overview

In NOMA, each user operates in the same band and at the same time where they are distinguished by their power levels. NOMA uses superposition coding at the transmitter such that the successive interference cancellation (SIC) receiver can separate the users both in the uplink and in the downlink channels. NOMA was proposed as a candidate radio access technology for 5G cellular systems.

Practical implementation of NOMA in cellular networks requires high computational power to implement real-time power allocation and successive interference cancellation algorithms. By 2020, 5G networks are targeted to be deployed, the computational capacity of both handsets and access points is expected to high enough to run NOMA algorithms. In this chapter, we present the fundamentals and capacity

limits of NOMA as a future radio access technology. The imperfectness in the SIC receiver and its impact on the overall capacity is also presented. We further demonstrate the improved energy and spectral efficiencies with NOMA over-conventional OFDMA.

Lately, Unmanned Aerial Vehicle (UAV) assisted mobile communication systems have been in the limelight for several deployment scenarios. UAVs can be instrumental in supporting the terrestrial wireless network by acting as a UAV Base Station (UAV-BS) to handle short-term erratic traffic demand in hotspots such as sports event as well as a concert or to mitigate congestion through data off-loading in access network. They can provide means to swiftly deploy recovery networks to connect first responder personnel in cases of natural calamity when the terrestrial network is partially or entirely malfunctioning or function as capacity and coverage enhancing relaying nodes and so on. It is conceivable that the UAV will provide additional support as either a stand-alone aerial BS or as a part of a heterogeneous network with the possibility of a multi-tier airborne cellular network. Irrespective of the deployment scenario, the inherited flexibility of UAV-assisted communication systems in terms of better channel conditions guaranteeing Line-of-Sight (LOS) links, faster deployment, and to find its parameters such as the best possible set of position and altitude to achieve better communication links with connected devices, can cater for the ever-rising diversified traffic demands whenever and wherever required.

The fruitful deployment of UAV based communication systems for 5G and beyond future wireless networks is highly involved in finding joint solutions to challenge of ubiquitous connectivity with both a multitude of devices in a spectral efficient way as well as with energy-efficient transmission and operation of the UAV-BS for maximized and harmonized coverage and capacity. It should be noted that suitable energy efficiency for the UAV-assisted communication system achieves paramount importance in the overall performance of the system. Efficient energy consumption results in enhanced airtime for the communication system, improving bits/Joules for a given energy level. Furthermore, coverage and capacity of an aerial cell are attributed to many factors such as the transmission power, antenna gains, UAV altitude, deployment environment, and prominently radio access technology. Recently, power domain NOMA reputations have climbed sharply as a fundamental solution to the challenges encompassing the next generation wireless networks. NOMA has been

proved to exhibit improved spectral efficiency, balanced and fair access as compared to OMA technologies, with the ability to cater for multiple devices in the same frequency, time, or code resource thus providing efficient access to massive connected devices. Furthermore, NOMA is also instrumental in reducing the interference by employing orthogonal resources by sharing a single beam between multiple users for intra-cluster access and using NOMA for inter-cluster access.

Current studies have focused on provisioning Air to Ground (A2G) communication services mainly through placement optimization under various viewpoints. Few works have considered a single UAV deployment scenario having zero interference to study optimal UAV altitude for maximized coverage. The performance of UAV based communication systems has also been addressed in for the under laid Device to Device (D2D) deployment scenario. This work assumed interference raised by D2D network nodes, without considering the presence of terrestrial BS. Additionally, there have been a few studies discussing the performance of NOMA for UAV based communication system. A NOMA enabled fixed-wing UAV deployment was proposed in to support coverage for ground users situated outside BS offloaded location. Some also suggested a multiple access mode selection (NOMA/OMA) based on conditions guaranteeing better outage probability for the ground users. An analysis of bit allocation and trajectory optimization for UAV mounted cloudlet for off-loading application was performed in, where NOMA demonstrated better energy conservation for the mobile users. Here, discusses a rather typical deployment scenario of an aerial BS, where the aspects of coverage and capacity are addressed considering performance thresholds for both cell-edge as well as the cell centre users. Furthermore, the implications of UAV altitude on coverage, capacity, and energy consumption considering different multiple access techniques that have been ignored in the literature also need to be addressed.

Thus, for a prolific deployment of UAV based communication systems, it is imperative to compare the performance of NOMA for UAV based communication systems to one based on OMA, in terms of optimized deployment, resource dispersal, performance, and energy efficiency. The main contributions of the report are as follows:

1) This proposes a power allocation scheme to maximize the sum-rate of the communication system with reducing energy expense for the UAV. The optimization problem is formulated as a function of the altitude of the UAV-BS, constrained to meet

or exceed the individual user-rates set forth by OMA for the same deployment scenario and target area.

2) Average rate and coverage under constraint is used as a tool to analyse the performance of the proposed schemes. Analytical and numerical analyses are presented for the proposed schemes and performance comparisons are also provided with altitude fixed OMA and NOMA schemes.

3) Results are presented for various target regions and deployment environments i.e., rural, urban, and dense urban. Clearly, the proposed scheme achieves better Sum - rate at a lower altitude which reduces the overall energy expenditure of the UAV.

CHAPTER 2

2. Non-orthogonal multiple access (NOMA)

We consider orthogonal frequency division multiplexing (OFDM) as the modulation scheme and NOMA as the multiple access scheme. In conventional 4G networks, as natural extension of OFDM, orthogonal frequency division multiple access (OFDMA) is used where information for each user is assigned to a subset of subcarriers. In NOMA, on the other hand, all of the subcarriers can be used by each user. **Figure 2.1** illustrates the spectrum sharing for OFDMA and NOMA for two users. The concept applies both uplink and downlink transmission.

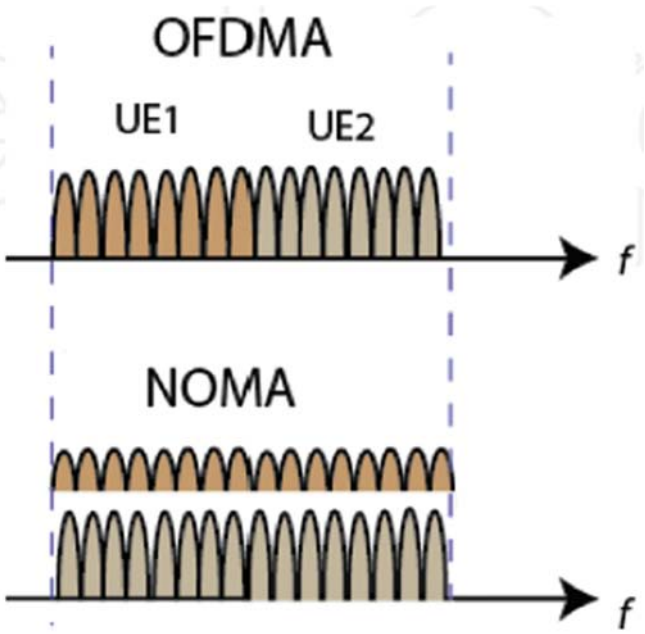

Figure 2.1. Spectrum sharing for OFDMA and NOMA for two users.

Superposition coding at the transmitter and successive interference cancellation (SIC) at the receiver makes it possible to utilize the same spectrum for all users. At the transmitter site, all the individual information signals are superimposed into a single waveform, while at the receiver, SIC decodes the signals one by one until it finds the desired signal. **Figure 2.2** illustrates the concept. In the illustration, the three information signals indicated with different colours are superimposed at the

transmitter. The received signal at the SIC receiver includes all these three signals. The first signal that SIC decodes is the strongest one while others as interference. The first decoded signal is then subtracted from the received signal and if the decoding is perfect, the waveform with the rest of the signals is accurately obtained. SIC iterates the process until it finds the desired signal.

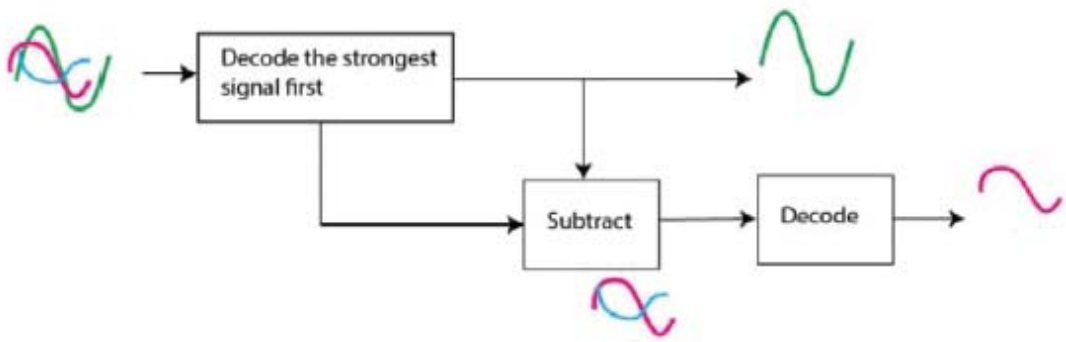

Figure 2.2. Successive interference cancellation.

The success of SIC depends on the perfect cancellation of the signals in the iteration steps. The transmitter should accurately split the power between the information waveforms and superimpose them. The methodology for power split differs for uplink and downlink channels.

2.1. NOMA for downlink

In NOMA downlink, the base station superimposes the information waveforms for its serviced users. Each user equipment (UE) employs SIC to detect their own signals. **Figure 2.3** shows a BS and K number of UEs with SIC receivers. In the network, it is assumed that the UE_1 is the closest to the base station (BS), and UE_k is the farthest. The challenge for BS is to decide how to allocate the power among the individual information waveforms, which is critical for SIC. In NOMA downlink, more power is allocated to UE located farther from the BS and the least power to the UE closest to the BS. In the network, all UEs receive the same signal that contains the information for all users. Each UE decodes the strongest signal first, and then subtracts the decoded signal from the received signal. SIC receiver iterates the subtraction until it finds its own signal. UE located close to the BS can cancel the signals of the farther

UEs. Since the signal of the farthest UE contributes the most to the received signal, it will decode its own signal first.

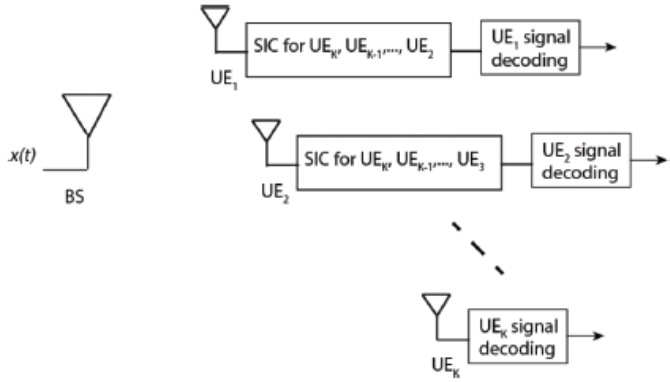

Figure 2.3. Downlink NOMA for K users.

The transmitted signal by the BS can be written as

$$x(t) = \sum_{k=1}^{K} \sqrt{\alpha_k P_T}\, x_k(t) \tag{1}$$

where $X_k(t)$ is the individual information conveying OFDM waveform, a_k is the power allocation coefficient for the UEk, and P_T is the total available power at the BS. The power allocated to each UEk then becomes $P_k = a_k P_T$. The power is allocated according to the distance of UEs to the BS: UE1 is the closest to the BS, so it is allocated the least power, whereas UEK is the farthest one, therefore it has the highest power.

The received signal at the UEk is

$$Y_k(t) = x(t) g_k + w_k(t) \tag{2}$$

where g_k is the channel attenuation factor for the link between the BS and the UE_k, and $w_k(t)$ is the additive white Gaussian noise at the UE_k with mean zero and density N_0 (W/Hz). Let us consider the farthest user first. The signal it decodes first will be its own signal since it is allocated the most power as compared the others. The signals for other users will be seen as interference. Therefore, the signal-to-noise ratio(SNR) for UEK can be written as

$$SNR_K = \frac{P_K g_K^2}{N_0 W + \sum_{i=1}^{K-1} P_i g_K^2} \quad (3)$$

Where W is the transmission bandwidth.

For the closest UE1, the last signal it decodes will be its signal. Assuming perfect cancellation, the SNR for UE1 becomes

$$SNR_1 = \frac{P_1 g_1^2}{N_0 W} \quad (4)$$

In general, for the UEk, the SNR becomes

$$SNR_k = \frac{P_k g_k^2}{N_0 W + \sum_{i=1}^{k-1} P_i g_k^2} \quad (5)$$

When NOMA is used, the throughput (bps) for each UE can be written as

$$R_k = W log_2 \left(1 + \frac{P_k g_k^2}{N + \sum_{i=1}^{k-1} P_i g_k^2}\right) \quad (6)$$

In OFDMA, on the other hand, UEs are assigned to a group of subcarriers in order to receive their information. When the total bandwidth and power are shared among the UEs equally, the throughput for each UE for OFDMA becomes

$$R_k = W_k log_2 \left(1 + \frac{P_k g_k^2}{N_k}\right) \quad (7)$$

where $W_k = W/K$ and $N_k = N_0 W_k$.

The sum capacity for both OFDMA and NOMA can be written as

$$R_T = \sum_{k=1}^{K} R_k \quad (8)$$

We further define fairness index as

$$F = \frac{(\sum R_k)^2}{K \sum R_k^2} \quad (9)$$

which indicates how fair the system capacity is shared among the UEs, that is, when *F* gets close to 1, the capacity for each UE gets close to each other.
We can set the objective of the power allocation mechanism as to maximize the sum capacity R_T under a fairness constraint for NOMA systems. The optimization problem is then formulated as

$$\underset{\alpha_k}{maximize} W log_2\left(1+\frac{P_k g_k^2}{N+\sum_{i=1}^{k-1} P_i g_k^2}\right) \quad subject\ to: \quad \sum_{k=1}^{K} P_k \leq P_T, \quad P_k \geq 0, \forall k, \quad F=F' \tag{10}$$

where F′ is the target fairness index in the network. The power allocation coefficients a_k for each UE_k can be obtained with exhaustive search.

2.2. NOMA for uplink

Uplink implementation of NOMA is slightly different than the downlink. **Figure 2.4** depicts a network that multiplexes *K* UEs in the uplink using NOMA. This time, BS employs SIC in order to distinguish the user signals.

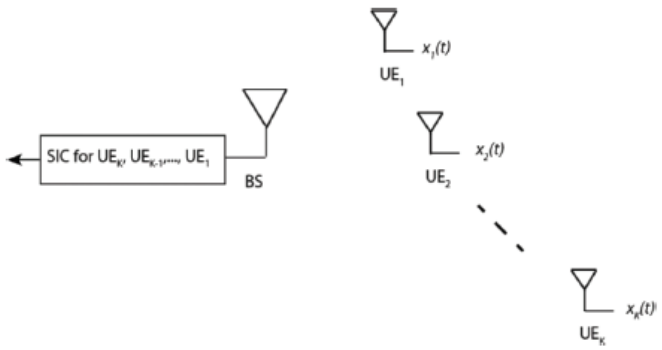

Figure 2.4. Uplink NOMA for K users.

In the uplink, the received signal by the BS that includes all the user signals is written as

$$y(t) = \sum_{k=1}^{K} x_k(t) g_k + w(t) \tag{11}$$

where g_k is the channel attenuation gain for the link between the BS and the UEk, $x_k(t)$ is the information waveform for the *k*th UE, and w(t) is the additive white Gaussian noise at the BS with mean zero and density N_0 (W/Hz). In the uplink, the UEs may again optimize their transmit powers according to their locations as in the downlink. However, here we assume that the users are well distributed in the cell coverage, and the received power levels from different users are already well separated. This assumption is more natural from practical point of view, since power optimization requires connection between all the UEs which may be difficult to implement. At the receiver, the BS implements SIC. The first signal it decodes will be the signal from the nearest user. The SNR for the signal for the UE1 can be written as, including others as interference,

$$R_1 = \frac{Pg_1^2}{N+\sum_{i=2}^{K} Pg_i^2} \tag{12}$$

where *P* is the transmission power of UEs and $N=N_0W$.

The last signal that the BS decodes is the signal for the farthest user UEK. Assuming perfect cancellation, the SNR for UE_K can be written as

$$SNR_K = \frac{Pg_K^2}{N} \tag{13}$$

Generally, for the *k*th UE, the SNR becomes,

$$SNR_k = 1 + \frac{Pg_k^2}{N+\sum_{i=k+1}^{K} Pg_i^2} \tag{14}$$

The throughput (bps) for each UE can be written as

$$R_k = Wlog_2\left(1 + \frac{Pg_k^2}{N+\sum_{i=k+1}^{K} Pg_i^2}\right) \tag{15}$$

In OFDMA, on the other hand, UEs are allocated orthogonal carriers in order to receive their information. When the total bandwidth and power are shared among the UEs equally, the throughput for each UE for OFDMA becomes

$$R_k = W_k log_2\left(1 + \frac{P_k g_k^2}{N_k}\right) \tag{16}$$

where W_k =W/K and N_k = N_0 W_k.

The sum capacity for both OFDMA and NOMA can be written as

$$R_T = \sum_{k=1}^{K} R_k \tag{17}$$

2.3. Imperfectness in NOMA

Our discussions so far in the previous sections assume perfect cancellation in the SIC receiver. In actual SIC, it is quite difficult to subtract the decoded signal from the received signal without any error. In this section, we revisit the NOMA concept with cancellation error in the SIC receiver.

Here, we consider the downlink only; however, the discussions can easily be extended for the uplink. Recall that SIC receiver decodes the information signals one by one iteratively to obtain the desired signal. In SIC, after decoding the signal, one should regenerate the original individual waveform in order to subtract it from the received signal. Although it is theoretically possible to complete this process without any error, in practice, it is expected to experience some cancellation error.

In downlink, the SNR for the *k*th user with cancellation error is written as

$$SNR_k = \frac{P_k g_k^2}{N_0 W + \sum_{i=1}^{k-1} P_i g_k^2 + \epsilon \sum_{i=k+1}^{K} P_i g_k^2} \tag{18}$$

where ε is cancellation error term that represents the remaining portion of the cancelled message signal. In the previous section, the third term in the denominator is not included since perfect cancellation is assumed there.

CHAPTER 3

3. Spectral efficiency and energy efficiency

3.1. Spectral efficiency

The analysis so far included the throughput performance of the network. In addition to Spectral Efficiency (SE) of NOMA, in this section, we analyse the Energy Efficiency (EE) of NOMA systems. In our analysis, we incorporate the static power consumption of the network due to the power amplifiers in addition to the power consumed for the information waveform. The total power consumption at the transmitter can be represented as the sum of the information signal power and the power consumed by the circuits (mainly by power amplifiers). Considering the downlink, the total power consumed by the BS can then be written as

$$P_{total} = P_T + P_{static} \tag{19}$$

where P_T is the total signal power as mentioned earlier and P_{static} is the power consumed by the circuitry.

3.2. Energy efficiency

Energy efficiency (EE) is defined as the sum rate over the total consumed power of the base station

$$EE = \frac{R_T}{P_{total}} = SE\frac{W}{P_{total}}\ (bits/joule) \tag{20}$$

where SE is the spectral efficiency (R_T/W) in terms of bps/Hz.

The energy efficiency and spectral efficiency relationship (EE-SE) in Shannon theory does not consider the power consumption of the circuit and consequently is monotonic where a higher SE always results in a lower EE. When the circuit power is considered,

the EE increases in the low SE region and decreases in the high SE region. The peak of the curve (or the corresponding derivative of the EE-SE relationship) is where the system has the maximum energy efficiency.

This point is called "*green point*". For a fixed P_{total}, the EE-SE relationship is linear with a positive slope of R_T/P_{total} where an increase in SE simultaneously results in an increase in EE. As we demonstrate in the next section, NOMA provides higher energy efficiency than OFDMA.

CHAPTER 4

4. Application of Non-Orthogonal Multiple Access in Unmanned Aerial Vehicle Assisted Communication

Before introducing the UAV networks with NOMA, we characterize the unique features of UAV networks first. Generally, UAV networks have the following characteristics:

- Path loss: Since there are usually not many obstacles in the air, we use a simplified model to assume that the line-of-sight (LOS) links between the UAVs and the users are dominated, which are significantly less effected by shadowing and fading. In more complicated practical scenarios, such as urban areas where buildings and other obstacles on the ground may block UAV flight and signal transmission, both LOS and non-line-of-sight (NLOS) links require to be considered.
- Mobility: When a UAV flies around, the coverage areas become various. Therefore, the UAV can support different ground users. For example, UAVs are capable of roaming above a group of users to enhance the channel conditions so as to provide high throughput.
- Agility: Based on the real-time requirements from the users, UAVs can be deployed quickly and their positions can be adjusted within a 3D space flexibly, which enables UAV networks to provide flexible and on-demand service to the ground users with lower costs compared to the terrestrial BS.

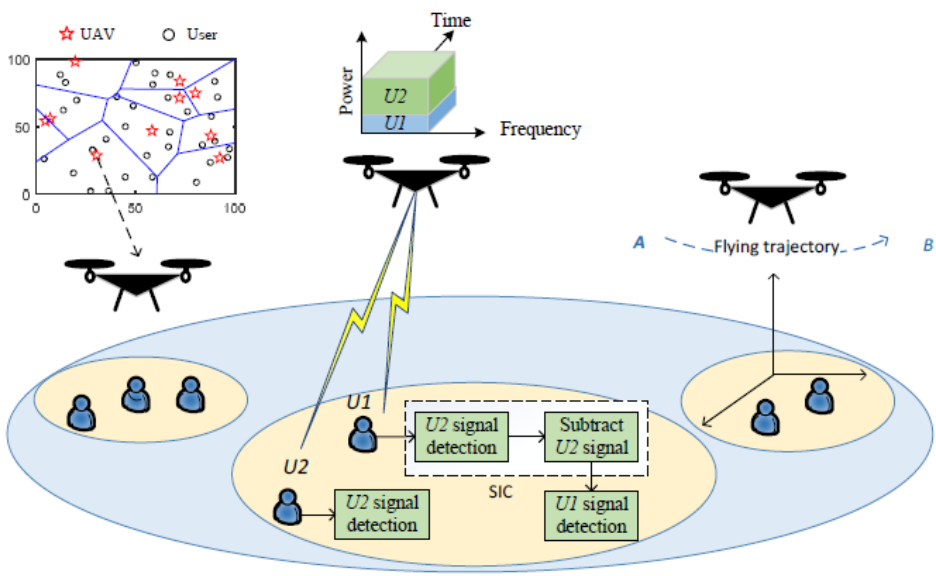

Figure 4.1. Illustration for NOMA-aided UAV networks.

4.1. SYSTEM AND CHANNEL MODEL

In this section the system model and A2G channel model are discussed.

4.1.1. System model

Consider a quasi-stationary low altitude rotary-wing UAV-BS deployed to provide wireless coverage in a disc-shaped circular region with a radius of *Rc* meters, where the radius of the cell is determined by the cell-edge user. **Fig. 4.2** represents a UAV-BS deployment scenario for two users located at points *R* and *S*, respectively, whereas the UAV-BS is hovering at altitude of *H* meters above the ground level, considered in the center of the target region, depicted by point *P* in **Fig. 4.2**. The vertical projection of the UAV-BS is represented by *Q* point. The distance between point *Q* and each user is represented by *Dj*. Then, the distance between the UAV-BS and each user is computed as:

$$X_j = \sqrt{D_j^2 + H^2}, j \in \{r, s\} \tag{21}$$

The elevation angle of UAV-BS with respect to each user is defined as:

$$\theta_j = arctan\left(\frac{H}{D_j}\right), j \in \{r, s\} \tag{22}$$

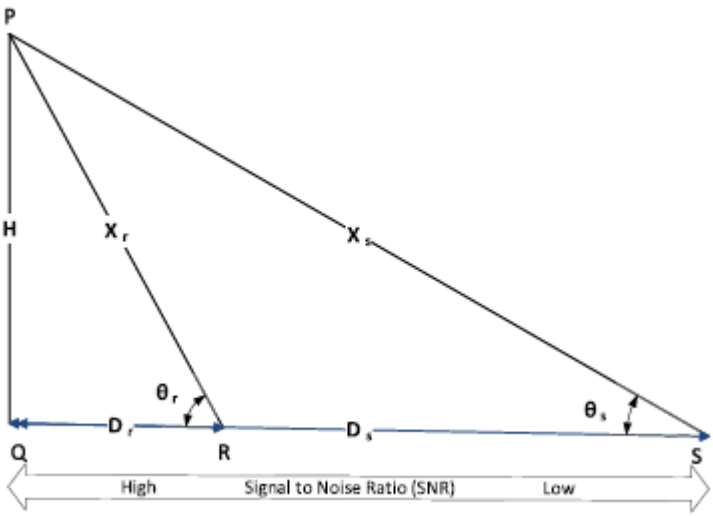

Figure 4.2. System model: A two-user UAV-assisted communication system, where PR and PS define the UAV-user links.

4.1.2. Channel model

Based on widely-adopted A2G channel model in the literature, the users can be classified as having either LOS link or strong Non-Line-Of-Sight (NLOS) link with UAV-BS. This classification is based on probabilistic model which depends on the environmental profile mainly defined by density and height of buildings in the coverage region as well as the relative distance between the user and UAV together, which defines the elevation angle. The effect of small scale fading is ignored in this model as probability of occurrence of weak multi-paths is much less than that of having LOS link or strong NLOS link. The probability of a user experiencing a LOS link with UAV-BS is expressed by :

$$Pr_j(LOS) = \frac{1}{1+\alpha exp(-\beta[\theta_j - \alpha])} \tag{23}$$

where α and β are constant values relating to the environmental profile of the coverage region such as rural, sub-urban, dense urban etc. The probability of user experiencing NLOS links is computed as:

$$Pr_j(NLOS) = 1 - Pr_j(LOS) \tag{24}$$

The Pr*j*(*LOS*) is an increasing function of the elevation angle and thus increasing the altitude of the UAV creates an opportunity for the ground user to have unobstructed LOS link with the UAV-BS. As presented in **Fig. 4.3**, the link between UAV and the ground users constitutes two distinctive scattering environments, namely low scattering and reflection close to the UAV as well as high scattering due to presence of man-made structures close to the ground users. Considering this fact, the total path loss is computed by free space path loss and excessive loss having higher value for NLOS links compared to LOS links due to excessive losses caused by reflection of the transmitted signals and shadowing which is contributed by objects obstructing the paths in the coverage region.

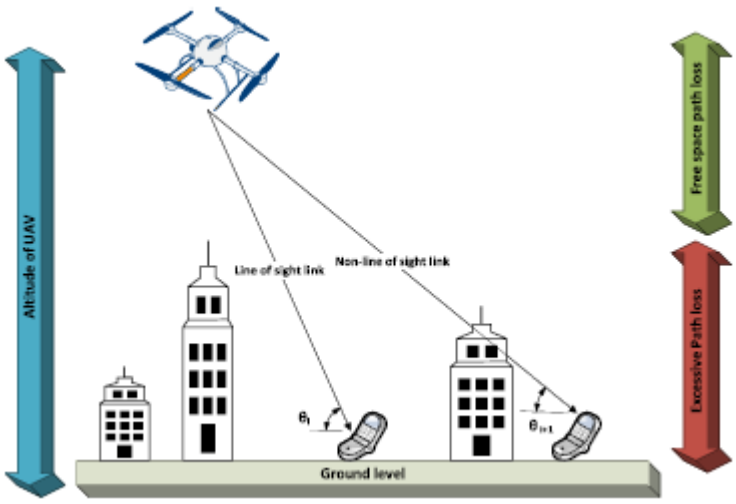

FIGURE 4.3. Excessive path loss model.

Thus, considering the Downlink (DL) transmission, the received power by *j th* user is given as:

$$P_{rx,j}(dB) = P_{tx}(dB) - L_j(dB) \tag{25}$$

where *Ptx* represents the transmitted power by the UAV-BS and *Lj* indicates the path loss for A2G channel between the UAV-BS and the *j th* user on the ground, computed as :

$$L_j = \begin{cases} 10\eta log(X_j) + x_{LOS}, & LOS\ link \\ 10\eta log(X_j) + x_{NLOS}, & NLOS\ link \end{cases} \quad (26)$$

where η denotes the path loss exponent. X*LOS* and X*NLOS* represent the excessive path losses of both LOS and NLOS links owing to shadow fades, respectively. Both terms comply with normal distribution, whose mean and variance are dependent on the elevation angle and environment dependent constant values. Typically, the knowledge of UAV and user location without having terrain map cannot warrant information about the type of link (LOS/NLOS) between the UAV and the user. Thus, the relationship in (25) is rewritten as *Prx*;*j*(*dB*) = *Ptx* (*dB*)-*Lj'*(*Rc*;*H*), where *Lj'*(*Rc*;*H*) defines the mean path loss considering probabilities for both LOS and NLOS UAV-user links computed as:

$$\overline{L}_j(R_c, H) = Pr_j(LOS)L_j(LOS) + Pr_j(NLOS)L_j(NLOS) \quad (27)$$

4.2. Energy Model

Zorbas *et al.* [25] drew an explicit relationship associating the energy consumption of rotary-wing UAV with its altitude and weight. According to the suggested model, the energy consumption of UAV at any time *T* can be given as *ET =mgH*, where *mg* is determined by the weight of the UAV *m* and acceleration of gravity *g* as well as *H* represents the altitude of the UAV at time *T* . The relationship between the altitude of UAV and its energy consumption has also been reported and proven through experiments in [26]_[28]. However, the model presented in [25] is simplistic and falls well short of acknowledging many factors affecting the overall energy consumption such as velocity, flight maneuvers, motor and blade profiles, etc. Ueyama *et al.* [27] and Franco and Buttazzo [28] also presented real measured data for different postures

of the UAV i.e. idling on the ground, ascending to and descending from a certain altitude, hovering, and moving in a straight flight. Based on the results, energy consumption increases dramatically to reach higher altitudes and hovering which usually consumes less energy among other maneuvers of the UAV, is also related to the hovering altitude. The total energy consumption of a UAV to reach a desired altitude *H* from the initial ground position and perform hovering for time *t* can be given as [28]:

$$E = E_{climb} + E_{hover} \tag{28}$$

$$= P_{climb} \frac{H}{v_{climb}} + P_{hover} t \tag{29}$$

where, *Pclimb* and *Phover* represent the power required by the UAV to climb and hover, respectively. Also, the velocity of ascending is denoted as V*climb* and *t* represents the flight duration. The relationship presented in (29) can be further elaborated based on the work presented by the authors in [29] suggesting that the UAV may attain high altitude for better coverage, by contrast with fixed wing UAV. This also leads to more energy consumption. The energy consumption model given in (29) can be rewritten as [29]:

$$E = \underbrace{P_{max}}_{P_{climb}} \left(\frac{H}{v_{climb}}\right) + \underbrace{(\psi + \Gamma H)t}_{P_{hover}} \tag{30}$$

Where ψ represents the minimum power needed to hover just over the ground, Γ denotes the motor speed multiplier, *Pmax* means the maximum power of the motor. The terms ψ and Γ depend on UAV weight and the characteristics of the motor, respectively. Energy consumption needed to lift UAV to an altitude *H* with velocity *Vclimb* is *Pmax*(*H*/*Vclimb*). Assuming optimized velocity for a given UAV design, a reduction in the operational altitude of the UAV allows further energy savings. Specifically, let *Ho* be the optimized altitude for the UAV given OMA. Then, the energy consumption *Eo* assuming OMA can be written as:

$$E_0 = P_{max}\left(\frac{H_0}{v_{climb}}\right) + (\psi + \Gamma H_0)t \tag{31}$$

Similarly, E_N defines the operational energy consumption of the UAV assuming H_N *as* the optimized altitude given NOMA :

$$E_N = P_{max}\left(\frac{H_N}{v_{climb}}\right) + (\psi + \Gamma H_N)t \tag{32}$$

Hence, the following difference equation can be used to compare the energy consumption of OMA and NOMA schemes:

$$E_0 - E_N = \Delta E = \left(\Gamma t + \frac{P_{max}}{v_{climb}}\right)\Delta h \tag{33}$$

where $\Delta h = HO - HN$.

As Γ, *Pmax*, *t*; *and V* can be considered constant values when UAVs with similar design specifications and velocity are deployed for both cases. $\Delta h > 0$ implies NOMA achieving better energy savings due to lower required altitude H_N .

4.3. Performance of downlink Orthogonal Multiple Access (OMA) at the optimal UAV altitude

In this section, the method of computing maximum sum-rate at the optimum UAV altitude for the proposed system model under OMA is discussed. The method assumes Time Division Multiple Access (TDMA) between two users, however, the concept can be easily extended to more number of users. This assumption brings OMA at par with NOMA for analysis purposes, considering the proposed scheme for 3GPP Long Term Evolution-Advanced (LTE-A), to group users by selecting two NOMA users within each group [30]. Later, the sum-rate and individual user-rates employing OMA are considered as bench marks and set as constraints in the study of NOMA viability of UAV-assisted communication systems. Assuming the system model, the channel between UAV-BS and the *jth* user on the ground is denoted by $h_j = 1/(1+L_j'(R_{C,H}))^{1/2}$ where the small-scale fading effect is ignored as the channel model

between the UAV and ground users is based on probabilistic LOS and NLOS links instead of the classical fading channel [19]. The channel capacity for any *user*$_j$ employing OMA is given as [32]:

$$R_j^{OMA} = \frac{1}{2}\log_2\left(1 + \gamma\left|h_j\right|^2\right) \ , \ j \in \{r, s\} \tag{34}$$

where γ and the constant factor 1/2 represents the transmit Signal to Noise Ratio (SNR) and equal distribution of time resource between the two users, respectively. The sum-rate is given as:

$$C_{OMA} = \frac{1}{2}\log_2(1 + \gamma|h_r|^2) + \frac{1}{2}\log_2(1 + \gamma|h_s|^2) \tag{35}$$

As the channel capacity is a function of the channel gains, the next step is to find the optimal altitude for a given distribution of users. As presented in [7], assume a UAV-BS transmitting signals in the DL with a transmission power of *Ptx* then the mean received power at the *j-th* user can be written as:

$$P_{rx,j}(dB) = P_{tx} - \overline{L}(R_c, H) \tag{36}$$

The optimum altitude of UAV-BS, *HO* with the minimum required transmission power can be calculated by solving [7]:

$$P_{rx,j}(dB) = P_{tx} - \overline{L}(R_c, H) \tag{37}$$

Additionally, it is trivial to verify that the *Rc* as a function of *H* is a concave function and if a local maxima exists, then the corresponding value of altitude of UAV-BS, *Ho* becomes the global optimum. It is conceivable that for a given fixed coverage radius *Rc*, a UAV-BS at *Ho* provides the best possible SNR for all terrestrial users, which leads to maximized sum-rate [7]. Once the optimal altitude *Ho* has been determined, individual user-rate for OMA is computed.

4.4 Performance of downlink Non-Orthogonal Multiple Access (NOMA)

In this section, the performance of the system under our considerations is maximized for the cases of capacity and altitude. An optimization problem for each case is formulated with minimum target rate, i.e. data rate achievable by OMA, being set as constraint. Sum-rate maximization as a function of power allocation coefficients (Altitude fixed as in OMA).

4.4.1. Altitude fixed NOMA sum-rate maximization

As channel gain is a decreasing function of the distance between the transmitter and the receiver, it is evidently stated that $|h_s|^2 <= |h_r|^2$ for the *s th* and *r th* user selected to utilize NOMA, 1 <=*s* <= *r*. Considering DL NOMA, the channel capacity for *s th* and *r th* users are given, respectively as [32]:

$$R_s^{NOMA} = log_2\left(1 + \frac{\omega_s|h_s|^2}{\omega_r|h_s|^2+1/\gamma}\right) \tag{38}$$

$$R_r^{NOMA} = log_2(1 + \omega_r\gamma|h_r|^2) \tag{39}$$

where ω_s and ω_r represent the power allocation coefficients for users *s* and *r*, respectively and $\omega_s = 1 - \omega_r$. The necessary condition for user *r* to successfully remove *s-th* user interference before the *r-th* user can detect its own message, given by $R_{r\to s}^{NOMA} \geq R_s^{NOMA}$, is always satisfied for $h_s|^2 <= |h_r|^2$, where $R_{r\to s}^{NOMA} = \log_2(1+\frac{\omega_s|h_r|^2}{\omega_r|h_r|^2+1/\gamma})$.
For NOMA that employs multiple access in the power domain, the potential gains can be achieved by allocating power to paired users based on instantaneous channel gains opposed to fixed power allocation scheme [12], [17], [32], which cannot always guarantee to meet Quality-of-Service (QoS) without thoughtfully adjusting various parameters [31], [33]. Additionally, the gains of NOMA can be weighed against OMA

only if the data rates achieved by NOMA are strictly better or at least equal to data rates achievable by OMA schemes [32], [34]. Thus, the problem of sum-rate maximization can be written as an optimization problem:

$$\max_{\omega_s,\omega_r} C^{NOMA} \tag{40}$$

$$subject\ to: constraint\ 1: R_{r,H_0}^{NOMA} \geq R_{r,H_0}^{OMA} \tag{41}$$

$$constraint\ 2: R_{s,H_0}^{NOMA} \geq R_{s,H_0}^{OMA} \tag{42}$$

$$constraint\ 3: \omega_s + \omega_r \leq 1 \tag{43}$$

Where $C^{NOMA} = R_s^{NOMA} + R_r^{NOMA}$. Hence the first two constraints ensure that NOMA strictly guarantees better or equivalent individual rates compared to ones achieved by OMA schemes. And the last constraint ensures the total transmitted power does not exceed the maximum allowed transmission power. Following the procedure for power allocation presented in [32], the user with higher channel gain is assumed to be the primary user. Thus, the lower bound of the power allocation factor ω_r using the relationship defined by *constraint* 1 is given as:

$$log_2(1 + \omega_r \gamma |h_r|^2) \geq \frac{1}{2} log_2(1 + \gamma |h_r|^2) \tag{44}$$

$$\omega_r \geq \frac{1}{y+1} \tag{45}$$

Where $y = (1 + \gamma |h_r|^2)^{1/2}$. Similarly, solving for *constraint* 2 by assuming weaker channel user as the primary user, the upper bound on ω_r is as follows:

$$log_2\left(1+\frac{\omega_s|h_s|^2}{\omega_r|h_s|^2+1/\gamma}\right) \geq \frac{1}{2}\log_2(1+\gamma|h_s|^2) \tag{46}$$

$$\omega_r \leq \frac{1}{z+1} \tag{47}$$

Where $z = (1+\gamma|h_s|^2)^{1/2}$. The upper and lower bounds for ω*r* can be combined by introducing two tuning coefficients μ1 and μ2 given as:

$$\boldsymbol{\omega_r = \frac{\mu_1}{y+1} + \frac{\mu_2}{z+1}} \tag{48}$$

where μ1=1- μ2. Thus, *constraints* 1 and 2 can be met simultaneously for any value of μ_i. Furthermore, these can be tuned to achieve trade-offs between sumrate maximization and fairness among users or to meet diversified QoS requirements such as for neighbourhood area networks applications in smart grid communication networks [35]. By using (38) and (39), *CNOMA* is given by:

$$C^{NOMA} = log_2(1+\omega_r\gamma|h_r|^2) + log_2\left(1+\frac{\omega_s|h_s|^2}{\omega_r|h_s|^2+1/\gamma}\right) \tag{49}$$

Equivalently,

$$C^{NOMA} = log_2(1+\omega_r\gamma|h_r|^2) + log_2\left(\frac{1+\gamma|h_s|^2}{1+\omega_r\gamma|h_s|^2}\right) \tag{50}$$

It can be observed in (30) that $\omega_r\gamma\ |h_s|^2 <= \omega_s\gamma\ |h_r|^2$ as $|h_s|^2 <= |h_r|^2$, thus the sum-rate for NOMA monotonically increases with increasing !*r* . Furthermore, as ω_r is an increasing function of μ2 and the maximum value of μ2 i.e. 1, maximizes the sum-rate of NOMA.

The solution to the optimization problem defined by (40)-(43) is given by:

$$C_{max}^{NOMA} = log_2\left(\frac{z^2+zy^2}{z+1}\right) \tag{51}$$

CHAPTER 5

5. Simulation and Results

5.1. Rate pairs

We assume that there are two users in the network for the sake of discussion and analyse the boundaries of the achievable rate regions for these two users. We consider a symmetric downlink channel so that the users are at equal distance to the BS. SNR1 = SNR2 = 10dB. **Figure 5.1** shows the boundaries of the achievable rate regions R1 and R1 for NOMA and OFDMA. As illustrated in **Figure 5.1**, NOMA achieves higher rate pairs than the OFDMA except at the corners points (where the rates are equal to the single user capacities). When the fairness is high, both users experience 1.6 bps/Hz throughputs with both NOMA and OFDMA. However, when the fairness is lower, both sum capacity and individual throughputs are higher with NOMA. **Figure 5.2** shows rate pairs when the channel is asymmetric, that is,SNR1 = 20dB and SNR2 = 0dB . NOMA achieves much higher rate pairs than OFDMA, particularly for the farther user, UE2.

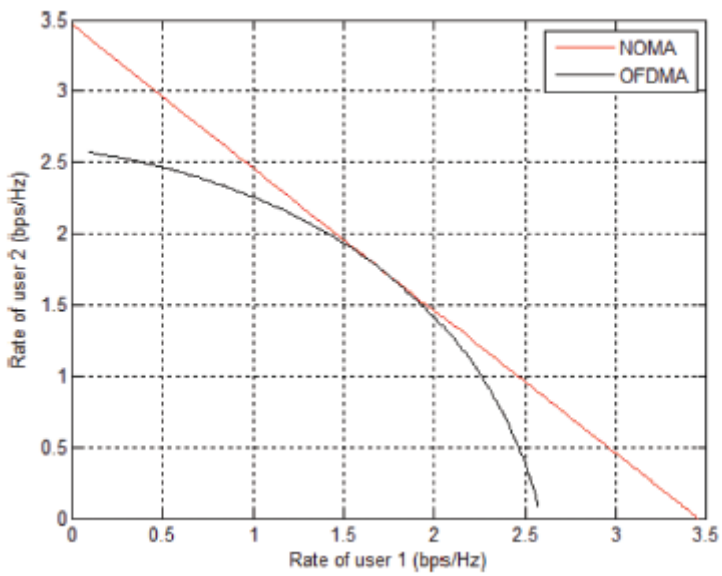

Figure 5.1. Rate pairs with OFDMA and NOMA for downlink NOMA, SNR1 = SNR2 = 10dB

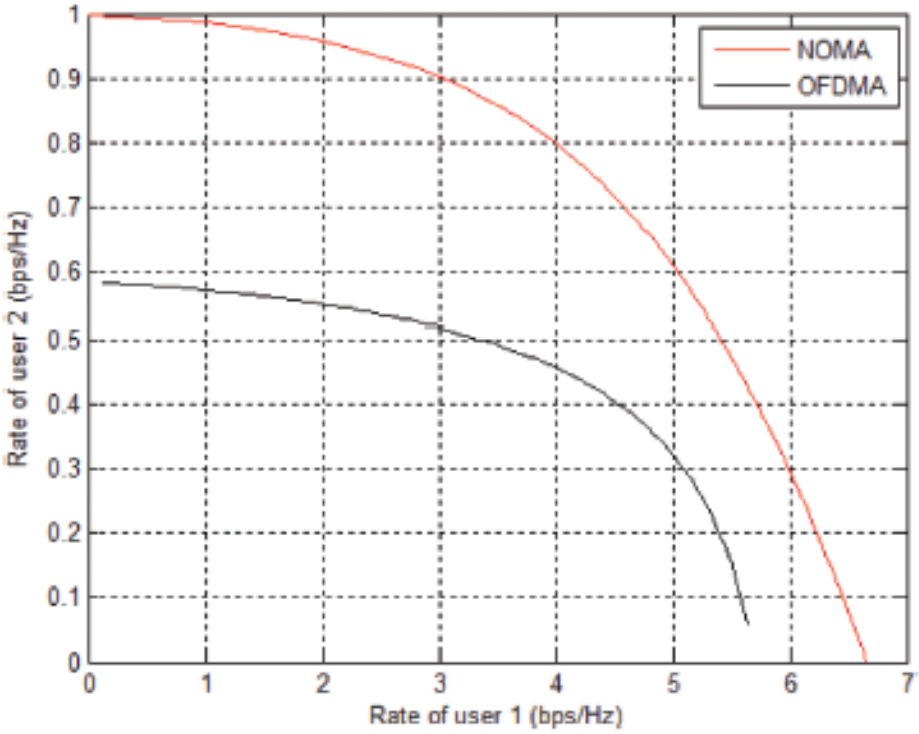

Figure 5.2. Rate pairs with OFDMA and NOMA for downlink NOMA, SNR1 = 20dB and SNR2 = 0dB.

5.2. Impact of imperfect cancellation

We repeat the same conditions for the asymmetric downlink channel in the previous section with imperfectness in SIC. The case for perfect cancellation is given as preference which is the same as the results in **Figure 5.2**. We then analyze the impact of imperfect cancellation by setting the cancellation error term (ε) at 1, 5 and 10%. For instance, when ε = 1%, UE1 cannot perfectly cancel the signal for UE2 in the first iteration, and 1% of the power of the second user's signal still remains as interference. When ε = 1%, the individual rate pairs and accordingly overall capacity slightly reduce. When ε = 10%, on the other hand, the reduction is more distinct.

5.3. SE-EE trade-off with NOMA

Here, we compare the EE and SE of NOMA with OFDMA. We again consider the downlink. The system bandwidth is taken as W = 5 MHz. The channel gains for UE1 and UE2 are, respectively, taken as $g_1^2 = -120$dB and $g_2^2 = -140$dB. Noise density N_0 is taken as −150 dBW/Hz. We assume that the static power consumption at the BS is P_{static} = 100W . **Figure 5.3** shows the obtained EE-SE curves for this setup. It is seen that NOMA achieves higher EE and SE than OFDMA system. The green-points occur for NOMA and OFDMA when P_T is at 17 W and 18W, respectively. At these points, both systems achieve their maximum EE. NOMA clearly outperforms OFDMA at green point and beyond for both EE and SE.

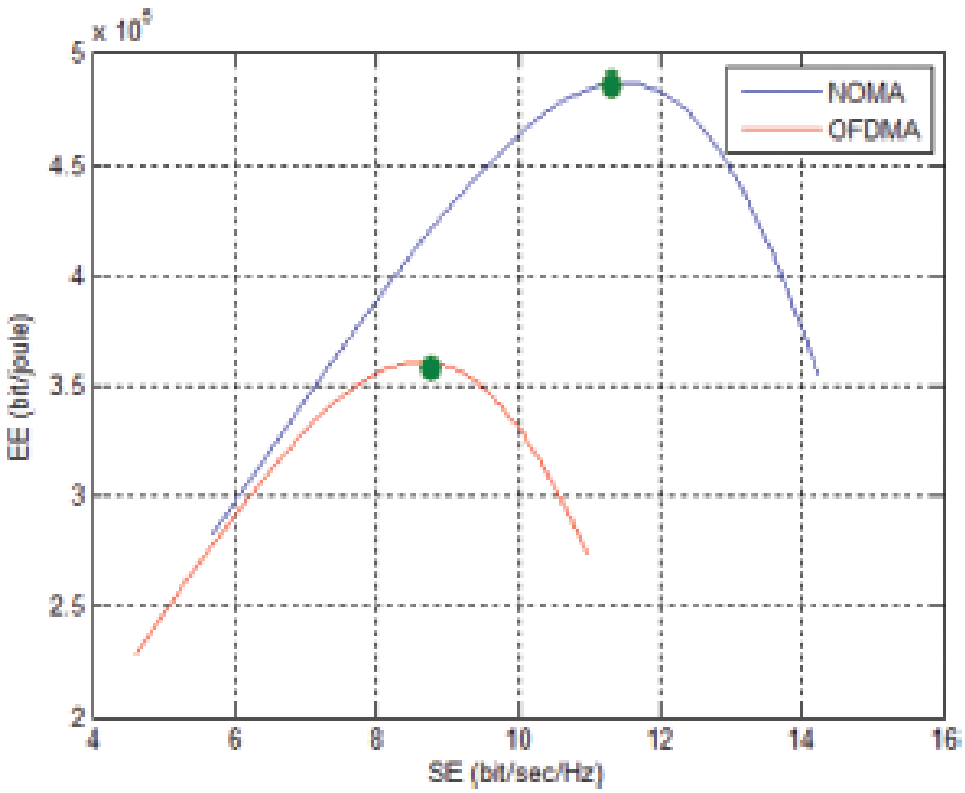

Figure 5.3. EE-SE trade-off curves for NOMA and OFDMA.

5.4 Optimization of NOMA

The simulations have been performed assuming urban, sub-urban and dense-urban environments with η = 2 for free-space path loss. The distance of the *r th* user for all simulations is given as *Dr* = 20 *m*, whereas the distance of *s th* cell-edge user, *Ds* = 60 *m*, The parameters for the considered environment are listed in table 1 (unless otherwise stated) [23].

Table 1. Simulation parameters for the considered environment.

Parameters	Sub-urban	Urban	Dense-urban
α	4.8860	9.6177	12.0870
β	0.4290	0.1581	0.1139
$\varkappa_{LOS}$	0.1	1	1.6
$\varkappa_{NLOS}$	21	20	23

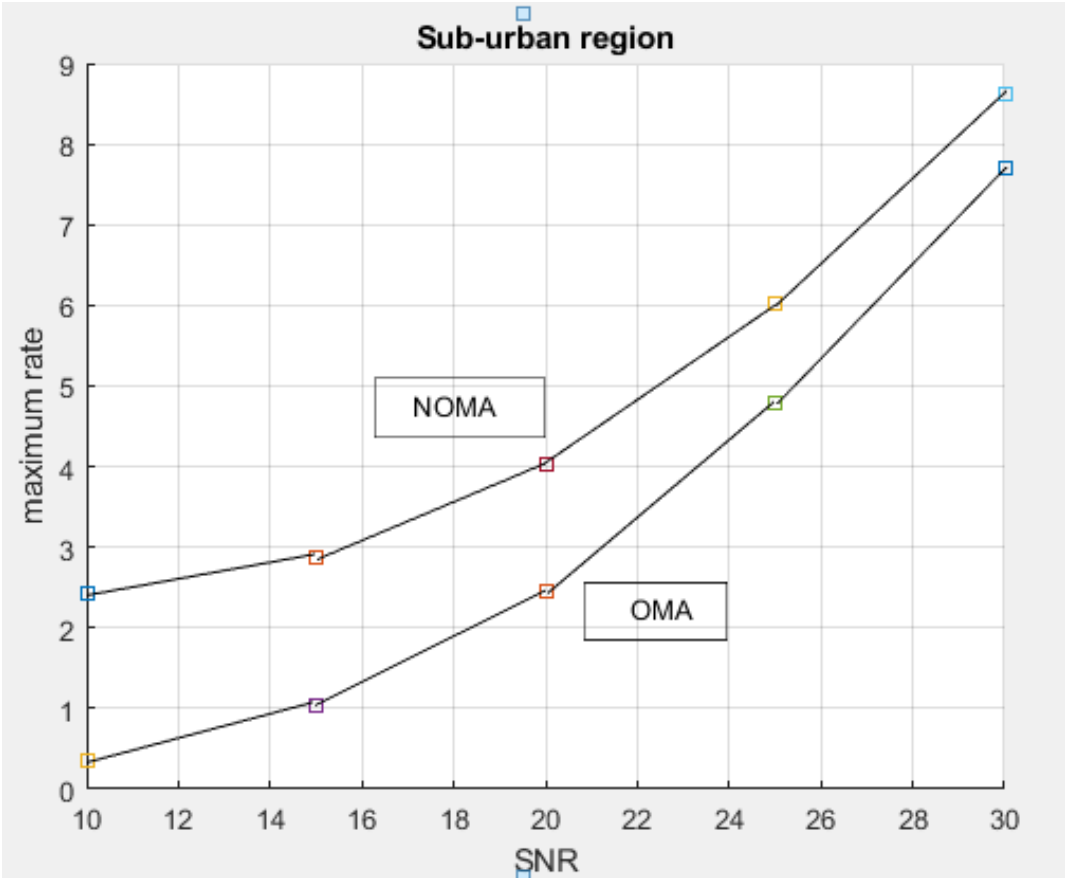

Figure 5.4. Average sum-rate in Sub-urban region for Rc = 60 m.

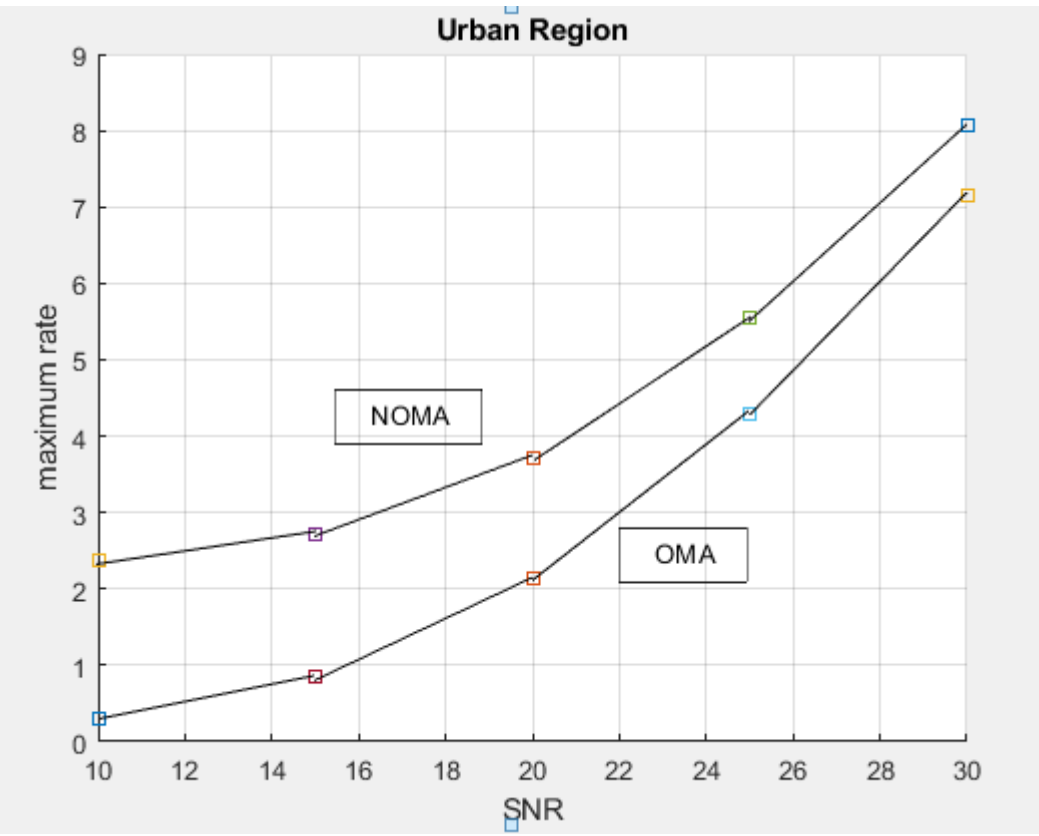

Figure 5.5. Average sum-rate in Urban region for Rc = 60 m.

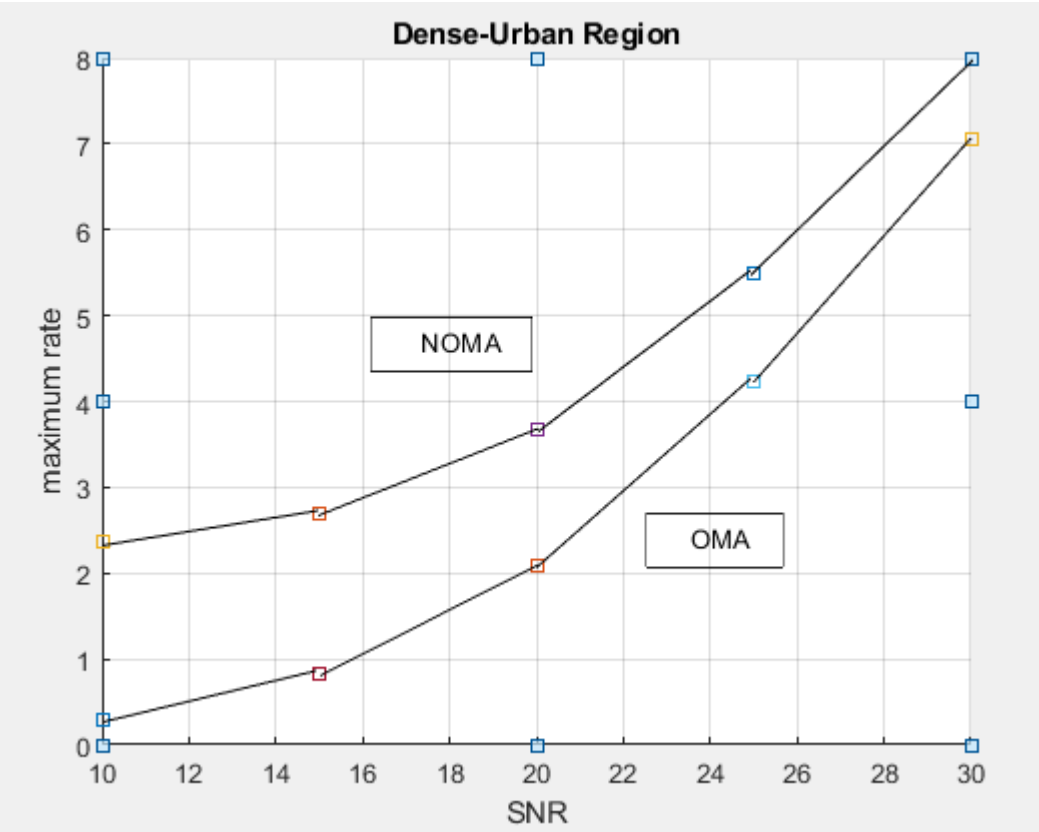

Figure 5.6. Average sum-rate in Dense-urban region for Rc = 60 m.

As energy consumption of the UAV-BS is an increasing function of its altitude, increasing Δh represents the increasing energy efficiency of NOMA compared to OMA. The higher probability of NLOS links for some users in the dense-urban environment causes larger difference between user channel gains. This results in much larger energy gain for dense-urban areas than to those for other areas, which is attributed to better NOMA gains for a user pair exhibiting the best and worst channel conditions. The energy efficiency of the proposed scheme is further clarified by comparing UAV energy consumption between OMA and NOMA. The lower required altitude to cover a given sub-urban area as compared to urban and dense-urban allows achieving higher energy efficiency. We can clearly see NOMA has better results in all the three regions than OMA in terms of sum-rate.

CHAPTER 6

6. Conclusion

We have seen the fundamentals of NOMA and demonstrated its superior performance over conventional OFDMA in terms of sum capacity, energy efficiency and spectral efficiency. We have further mentioned the impact of imperfectness at the SIC receiver on the system performance. With its distinct features, NOMA stays as the strongest candidate for the future 5G networks.

We also investigated an account of NOMA's applicability for UAV-assisted communication systems. The crucial need to transmit more bits per joule inspired the proposed scheme for sum-rate maximization with reduced energy consumption. Taken together, presented results manifests that NOMA performs better than OMA while fulfilling individual user rate constraint for both users.

Bibliography

[1] A. M. Hayajneh, S. A. R. Zaidi, D. C. McLernon, and M. Ghogho, ``Drone empowered small cellular disaster recovery networks for resilient smart cities,'' in *Proc. IEEE Int. Conf. Sens., Commun. Netw. (SECON Workshops)*, Jun. 2016, pp. 1_6.

[2] I. Bor-Yaliniz and H. Yanikomeroglu, ``The new frontier in RAN heterogeneity: Multi-tier drone-cells,'' *IEEE Commun. Mag.*, vol. 54, no. 11, pp. 48_55, Nov. 2016.

[3] Y. Zeng *et al.*, ``Throughput maximization for UAV-enabled mobile relaying systems,'' *IEEE Trans. Commun.*, vol. 64, no. 12,
pp. 4983_4996, Dec. 2016.

[4] S. Chandrasekharan *et al.*, ``Designing and implementing future aerial communication networks,'' *IEEE Commun. Mag.*, vol. 54, no. 5, pp. 26_34, May 2016.

[5] R. I. Bor-Yaliniz, A. El-Keyi, and H. Yanikomeroglu, ``Efficient 3-D placement of an aerial base station in next generation cellular networks,'' in *Proc. IEEE Int. Conf. Commun. (ICC)*, May 2016, pp. 1_5.

[6] M. Mozaffari,W. Saad, M. Bennis, and M. Debbah, ``Efficient deployment of multiple unmanned aerial vehicles for optimal wireless coverage,'' *IEEE Commun. Lett.*, vol. 20, no. 8, pp. 1647_1650, Aug. 2016.

[7] M. Mozaffari, W. Saad, M. Bennis, and M. Debbah, ``Drone small cells in the clouds: Design, deployment and performance analysis,'' in *Proc. IEEEGlobal Commun. Conf. (GLOBECOM)*, Dec. 2015, pp. 1_6.

[8] Y. Zeng, R. Zhang, and T. J. Lim, ``Wireless communications with unmanned aerial vehicles: Opportunities and challenges,'' *IEEE Commun. Mag.*, vol. 54, no. 5, pp. 36_42, May 2016.

[9] S. Ali, E. Hossain, and D. I. Kim, ``Non-orthogonal multiple access (NOMA) for downlink multiuser MIMO systems: User clustering,
beamforming, and power allocation,'' *IEEE Access*, vol. 5, pp. 565_577, Mar. 2017.

[10] Y. Sun, D. W. K. Ng, Z. Ding, and R. Schober, ``Optimal joint power and subcarrier allocation for full-duplex multicarrier nonorthogonal multiple access systems,'' *IEEE Trans. Commun.*, vol. 65, no. 3, pp. 1077_1091, Mar. 2017.

[11] S. M. R. Islam, N. Avazov, O. A. Dobre, and K.-S. Kwak, ``Power-domain non-orthogonal multiple access (NOMA) in 5G systems: Potentials and challenges,'' *IEEE Commun. Surveys Tuts.*, vol. 19, no. 2, pp. 721_742, 2nd Quart., 2017.

[12] Z. Ding *et al.*, ``Application of non-orthogonal multiple access in LTE and 5G networks,'' *IEEE Commun. Mag.*, vol. 55, no. 2, pp. 185_191, Feb. 2017.

[13] S. Lee, D. B. da Costa, Q.-T. Vien, T. Q. Duong, and R. T. de Sousa, ``Non-orthogonal multiple access schemes with partial relay selection,'' *IET Commun.*, vol. 11, no. 6, pp. 846_854, 2017.

[14] Z. Yang, Z. Ding, P. Fan, and N. Al-Dhahir, ``The impact of power allocation on cooperative non-orthogonal multiple access networks with SWIPT,'' *IEEE Trans. Wireless Commun.*, vol. 16, no. 7, pp. 4332_4343, Jul. 2017.

[15] Z. Chen, Z. Ding, X. Dai, and R. Zhang, ``An optimization perspective of the superiority of noma compared to conventional OMA,'' *IEEE Trans. Signal Process.*, vol. 65, no. 19, pp. 5191_5202, Oct. 2017.

[16] P. Xu and K. Cumanan, ``Optimal power allocation scheme for nonorthogonal multiple access with _-fairness,'' *IEEE J. Sel. Areas Commun.*, vol. 35, no. 10, pp. 2357_2369, Oct. 2017.

[17] M. S. Ali, H. Tabassum, and E. Hossain, ``Dynamic user clustering and power allocation for uplink and downlink non-orthogonal multiple access (NOMA) systems,'' *IEEE Access*, vol. 4, pp. 6325_6343, 2016.

[18] Z. Chen, Z. Ding, and X. Dai, ``Beamforming for combating inter-cluster and intra-cluster interference in hybrid NOMA systems,'' *IEEE Access*, vol. 4, pp. 4452_4463, Aug. 2016.

[19] M. Mozaffari, W. Saad, M. Bennis, and M. Debbah, ``Unmanned aerial vehicle with underlaid device-to-device communications: Performance and tradeoffs,'' *IEEE Trans. Wireless Commun.*, vol. 15, no. 6, pp. 3949_3963, Jun. 2016.

[20] A. Al-Hourani, S. Kandeepan, and S. Lardner, ``Optimal LAP altitude for maximum coverage,'' *IEEE Wireless Commun. Lett.*, vol. 3, no. 6, pp. 569_572, Dec. 2014.

[21] P. K. Sharma and D. I. Kim, ``UAV-enabled downlink wireless system with non-orthogonal multiple access,'' in *Proc. IEEE GlobecomWorkshops (GC Wkshps)*, Dec. 2017, pp. 1_6.

[22] S. Jeong, O. Simeone, and J. Kang, ``Mobile edge computing via a UAV mounted cloudlet: Optimization of bit allocation and path planning,'' *IEEE Trans. Veh. Technol.*, vol. 67, no. 3, pp. 2049_2063, Mar. 2018.

[23] A. Al-Hourani, S. Kandeepan, and A. Jamalipour, ``Modeling air-to-ground path loss for low altitude platforms in urban environments,'' in *Proc. IEEE Global Commun. Conf. (GLOBECOM)*, Dec. 2014, pp. 2898_2904.
[24] Q. Feng, J. McGeehan, E. K. Tameh, and A. R. Nix, ``Path loss models for air-to-ground radio channels in urban environments,'' in *Proc. IEEE 63rd Veh. Technol. Conf.*, vol. 6. May 2006, pp. 2901_2905.
[25] D. Zorbas, T. Raza_ndralambo, D. P. P. Luigi, and F. Guerriero, ``Energy efficient mobile target tracking using flying drones,'' *Proc. Comput. Sci.*, vol. 19, pp. 80_87, Jun. 2013.
[26] Y. Zhou, N. Cheng, N. Lu, and X. S. Shen, ``Multi-UAV-aided networks: Aerial-ground cooperative vehicular networking architecture,'' *IEEE Veh. Technol. Mag.*, vol. 10, no. 4, pp. 36_44, Dec. 2015.
[27] J. Ueyama *et al.*, ``Exploiting the use of unmanned aerial vehicles to provide resilience in wireless sensor networks,'' *IEEE Commun. Mag.*, vol. 52, no. 12, pp. 81_87, Dec. 2014.
[28] C. Di Franco and G. Buttazzo, ``Energy-aware coverage path planning of UAVs,'' in *Proc. IEEE ICARSC*, Apr. 2015, pp. 111_117.
[29] D. Zorbas, L. Di Puglia Pugliese, T. Raza_ndralambo, and F. Guerriero, ``Optimal drone placement and cost-ef_cient target coverage,'' *J. Netw. Comput. Appl.*, vol. 75, pp. 16_31, Nov. 2016.
[30] H. Lee, S. Kim, and J.-H. Lim, ``Multiuser superposition transmission (MUST) for LTE-A systems,'' in *Proc. IEEE Int. Conf. Commun. (ICC)*, May 2016, pp. 1_6.
[31] Z. Ding, Z. Yang, P. Fan, and H. V. Poor, ``On the performance of non-orthogonal multiple access in 5G systems with randomly deployed users,'' *IEEE Signal Process. Lett.*, vol. 21, no. 12, pp. 1501_1505, Dec. 2014.
[32] Z. Yang, Z. Ding, P. Fan, and N. Al-Dhahir, ``A general power allocation scheme to guarantee quality of service in downlink and uplink NOMA systems,'' *IEEE Trans. Wireless Commun.*, vol. 15, no. 11, pp. 7244_7257, Nov. 2016.
[33] Z. Ding *et al.*, ``Impact of user pairing on 5G nonorthogonal multiple access downlink transmissions,'' *IEEE Trans. Veh. Technol.*, vol. 65, no. 8, pp. 6010_6023, Aug. 2016.
[34] Z. Ding, F. Adachi, and H. V. Poor, ``The application of MIMO to non-orthogonal multiple access,'' *IEEE Trans. Wireless Commun.*, vol. 15, no. 1, pp. 537_552, Jan. 2016.
[35] S. Alam, M. F. Sohail, S. A. Ghauri, I. M. Qureshi, and N. Aqdas, ``Cognitive radio based smart grid communication network,'' *Renew. Sustain. Energy Rev.*, vol. 72, pp. 535_548, May 2017.
[36] R. H. Byrd, M E. Hribar, and J. Nocedal, ``An interior point algorithm for large-scale nonlinear programming,'' *SIAM J. Optim.*, vol. 9, no. 4, pp. 877_900, 1999.
[37] M. Alzenad, A. El-Keyi, F. Lagum, and H. Yanikomeroglu, ``3-D Placement of an unmanned aerial vehicle base station (UAV-BS) for energy efficient maximal coverage,'' *IEEE Wireless Commun. Lett.*, vol. 6, no. 4, pp. 434_437, Aug. 2017.

THANK YOU !